Dose-Related Side Effects of Intravitreal Injections of Humanized Anti-Vascular Endothelial Growth Factor in Rats: Glial Cell Reactivity and Retinal Ganglion Cell Loss

Ana Martínez-Vacas, Johnny Di Pierdomenico, Ana María Gómez-Ramirez, Manuel Vidal-Sanz, María P. Villegas-Pérez, and Diego García-Ayuso

Grupo de Investigación Oftalmología Experimental, Departamento de Oftalmología, Optometría, Otorrinolaringología y Anatomía Patológica, Facultad de Medicina, Universidad de Murcia, Instituto Murciano de Investigación Biosanitaria (IMIB), Campus de Ciencias de la Salud, Murcia, España

Correspondence: Diego García-Ayuso, Laboratorio de Oftalmología Experimental, Instituto Murciano de Investigación Biosanitaria-Virgen de la Arrixaca, Edificio LAIB Planta 5ª, Carretera Buenavista s/n, El Palmar, Murcia 30120, Spain; diegogarcia@um.es.
María P. Villegas-Pérez, Laboratorio de Oftalmología Experimental, Instituto Murciano de Investigación Biosanitaria-Virgen de la Arrixaca, Edificio LAIB Planta 5ª, Carretera Buenavista s/n, El Palmar, Murcia 30120, Spain; mpville@um.es.

AMV and JDP are joint first authors. MPVP and DGA are joint last and corresponding authors.

Received: October 10, 2023
Accepted: March 9, 2024
Published: April 4, 2024

Citation: Martínez-Vacas A, Di Pierdomenico J, Gómez-Ramirez AM, Vidal-Sanz M, Villegas-Pérez MP, García-Ayuso D. Dose-related side effects of intravitreal injections of humanized anti-vascular endothelial growth factor in rats: Glial cell reactivity and retinal ganglion cell loss. *Invest Ophthalmol Vis Sci.* 2024;65(4):10. https://doi.org/10.1167/iovs.65.4.10

Purpose. In a previous study, we documented that the Intravitreal injections (IVIs) of bevacizumab in rats caused a retinal inflammatory response. We now study whether the IVI of other humanized anti-VEGF: ranibizumab and aflibercept also cause an inflammatory reaction in the rat retina and if it depends on the dose administered. Finally, we study whether this reaction affects retinal ganglion cell (RGC) survival.

Methods. Albino Sprague–Dawley rats received a single IVI of 5 µL of PBS or ranibizumab or aflibercept at the concentration used in clinical practice (10 µg/µL or 40 µg/µL) or at a lower concentration (0.38 µg/µL and 1.5 µg/µL) calculated to obtain within the rat eye the same concentration as in the human eye in clinical practice. Others received a single 5 µL IVI of a polyclonal goat anti-rat VEGF (0.015 µg/µL) or of vehicle (PBS). Animals were processed 7 days or 1 month later. Retinal whole mounts were immunolabeled for the detection of microglial, macroglial, RGCs, and intrinsically photosensitive RGCs (ipRGCs). Fluorescence and confocal microscopy were used to examine retinal changes, and RGCs and ipRGCs were quantified automatically or semiautomatically, respectively.

Results. All the injected substances including the PBS induced detectable side effects, namely, retinal microglial cell activation and retinal astrocyte hypertrophy. However, there was a greater microglial and macroglial response when the higher concentrations of ranibizumab and aflibercept were injected than when PBS, the antibody anti-rat VEGF and the lower concentrations of ranibizumab or aflibercept were injected. The higher concentration of ranibizumab and aflibercept resulted also in significant RGC death, but did not cause appreciable ipRGC death.

Conclusions. The IVI of all the substances had some retinal inflammatory effects. The IVI of humanized anti-VEGF to rats at high doses cause important side effects: severe inflammation and RGC death, but not ipRGC death.

Keywords: microglia, macroglia, retina, RGC, ipRGC, vascular endothelial growth factor, inflammation

The VEGFs are a family of proangiogenic factors that play a major role in vascular and retinal homeostasis.[1] When acting upon their receptors, VEGFs enhance vessel endothelial cell survival and vascular permeability and promote endothelial cell proliferation and migration.[2] However, these factors may also act as mediators in various diseases that promote angiogenesis, blood–retinal barrier breakdown,[3] tumor growth,[4] and activation of inflammation.[5–7] In humans, several proteins that act as ligands for VEGF receptors have been identified, including VEGF-A, VEGF-B, VEGF-C, VEGF-D, and placental growth factor.[3,7] VEGF-A is considered the main factor in physiological and pathological angiogenesis.[8] Increased VEGF is believed to be important in the pathogenesis of various eye diseases, including neovascular AMD, posterior uveitis, endophthalmitis, myopic choroidal neovascularization, macular edema, and diabetic retinopathy, all of which are leading causes of irreversible blindness worldwide.[7,9]

To counteract the deleterious effects of VEGF in various diseases, factors that block VEGF by binding to or trapping VEGF protein receptors on the surface of endothelial cells, also known as anti-VEGF factors, have been synthesized for clinical use and used in ophthalmic diseases. The first was bevacizumab (Avastin, Roche, Basel, Switzerland),

which impeded angiogenesis and was first approved for cancer treatment.[10–12] Subsequently, pegaptanib (Macugen, Bausch & Lomb, Laval, Canada) became the first anti-VEGF drug specifically designed for ophthalmic use and approved for AMD treatment.[13] This anti-VEGF agent selectively binds to and blocks the activity of the extracellular VEGF-A165 isoform, the most potent and abundant VEFG A isoform.[3] However, it was later replaced by more effective anti-VEGF drugs, such as ranibizumab and aflibercept,[14] which inhibit all VEGF-A isoforms. Ranibizumab (Lucentis, Novartis, Camberley, UK) is a humanized monoclonal antibody derived from bevacizumab that has been approved for wet AMD treatment.[15,16] The recombinant VEGF-trap aflibercept (Eylea, Bayer, SA, Barcelona, Spain) has greater affinity for binding all forms of VEFG-A, P1GF-1, and P1GF2 when compared with ranibizumab and bevacizumab. At present, other drugs such as brolucizumab are available. All of these modern anti-VEGFs are humanized to mitigate the antiglobulin response that could arise from interspecies use,[17,18] thus improving their beneficial effects against human diseases.[18,19]

The intravitreal injection (IVI) of anti-VEGF factors has become one of the most effective used treatments in retinal vascular diseases.[3,20–23] Intravitreal administration of these factors allows their direct delivery to the retina while partially avoiding systemic absorption, thereby minimizing possible systemic side effects.[24–27] Although intravitreal anti-VEGF therapy has been documented to have few adverse effects,[3,28] both systemic and local, it is not risk free.[21,23,29–31] Additionally, given the limited duration of anti-VEGF drug effects, ocular therapy typically requires repeated IVI,[32–35] thereby increasing the likelihood of adverse effects.[29,36,37] However, little is known about the potential local side effects of the IVI of different anti-VEGF drugs injected at different doses.[38] Although the IVI of humanized anti-VEGF factors in humans is generally safe and nontoxic at standard therapeutic doses,[39,40] preclinical studies have indicated that the IVI of humanized anti-VEGF drugs in nonhuman subjects may yield adverse retinal effects in a dose-related manner.[37] A previous study conducted in our laboratory[36] demonstrated that the IVI induces microglial and macroglial responses in the rat retina, the severity of which varies with the injected agent. Humanized anti-VEGF drugs may contribute to metabolic and molecular changes in human Müller cells in vitro,[41,42] glial fibrillary acidic protein (GFAP) overexpression in rabbits,[43] and rats eyes,[36] and rat primary retinal cultures.[44] This reaction may vary depending on the specific drug used.[36,45] However, it remains unclear whether these potential side effects affect the survival of retinal neurons.[46–49] This point raises the question of whether the differences in retinal glial cell reactivity are attributable to the use of humanized anti-VEGF in other animal species or to the concentration used.

In this study, we analyze the survival of two different populations of retinal ganglion cells (RGCs), the general population and the intrinsically photosensitive RGCs (ipRGCs), and glial reactivity in rats following the IVI of the two of the most commonly used human anti-VEGFs at present: ranibizumab (Novartis), and aflibercept (Bayer) at two different concentrations: the concentration used in humans and a lower concentration calculated to obtain within the rat eye the same concentration as in the human eye in clinical practice. We also compared the effects of these substances with those obtained after the IVI of a goat polyclonal anti-rat VEGF antibody or vehicle.

Methods

Animal Handling and Groups

Adult female albino Sprague–Dawley rats ($n = 224$) weighing approximately 180 to 220 g were used. The rats were bred and maintained in the Experimental Animal Facility of the University of Murcia under controlled light (12-hour light-dark cycles with light intensity within the cages ranging from 5 to 30 lux) and temperature conditions (23°C–24°C), and with access to food and water ad libitum.

The animals were treated according to the current European and national regulations and, specifically, according to Directive 86/609/EEC, 2010/63/EU on the protection of animals used for scientific purposes, the R.D.1201/2005 on the protection of animals used for experimental and other scientific purposes, the Law 32/2007 for the care of animals, in their exploitation, transport, experimentation, and slaughter, and the ARVO guidelines for the use of animals in ophthalmic and visual system experimentation.

The IVIs (see IVIs) were performed under general anesthesia, for which a mixture of ketamine (70 mg/kg, Ketolar; Parke-Davies, SL, Barcelona, Spain) and xylazine (10 mg/kg, Rompun; Bayer) was injected intraperitoneally. After the IVIs, the rats were placed in their cages, and tobramycin ointment (Tobrex, Alcon S.A., Barcelona, Spain) was applied over the cornea to prevent corneal desiccation.

The animals were divided into different experimental groups. There were twelve animals in the naïve group that did not receive any treatment, twenty-four animals in the PBS group and forty animals in each of the groups that received IVI of the anti-VEGF factors. Half of the animals in each group were processed 7 days or 1 month after the IVI (Fig. 1; see IVIs). At each survival period, one-half of the animals were immunolabeled with antibodies directed to glial cells and half with antibodies directed to ganglion cells (see below, Immunohistofluorescence).

IVIs

The IVIs were performed only in the left eye following previously described methods.[36,50–52] Briefly, injections were performed through the superotemporal sclera at approximately 1–2 mm from the limbus using a Hamilton microsyringe (26G needle, Hamilton 701 N; Esslab, Benfleet, UK). The needle was introduced into the eye and directed to the vitreous core where, under direct visualization through the operating microscope, 5 µL of different substances (see next paragraph) were injected slowly to avoid injuring the lens or other ocular structures.

The following substances were injected in the different experimental groups: (1) PBS (Sigma Aldrich, Madrid, Spain); (2) ranibizumab (humanized anti-VEGF, Lucentis, Novartis) at two different concentrations: the human clinical concentration (higher concentration: 10 µg/µL) and a lower concentration (0.38 µg/µL) (see next paragraph); (3) aflibercept (humanized anti-VEGF, Bayer) at two different concentrations: the human clinical concentration (higher concentration; 40 µg/µL) and a lower concentration (1.5 µg/µL; see next paragraph); and (4) goat polyclonal anti-rat $VEGF_{164}$ diluted in PBS (15 µg/mL = 0, 015 µg/µL; MGC70609; Leinco Technologies, Inc., St. Louis, MO, USA).

Although the IVI volume was kept constant at 5 µL in all groups, two different concentrations of the two humanized

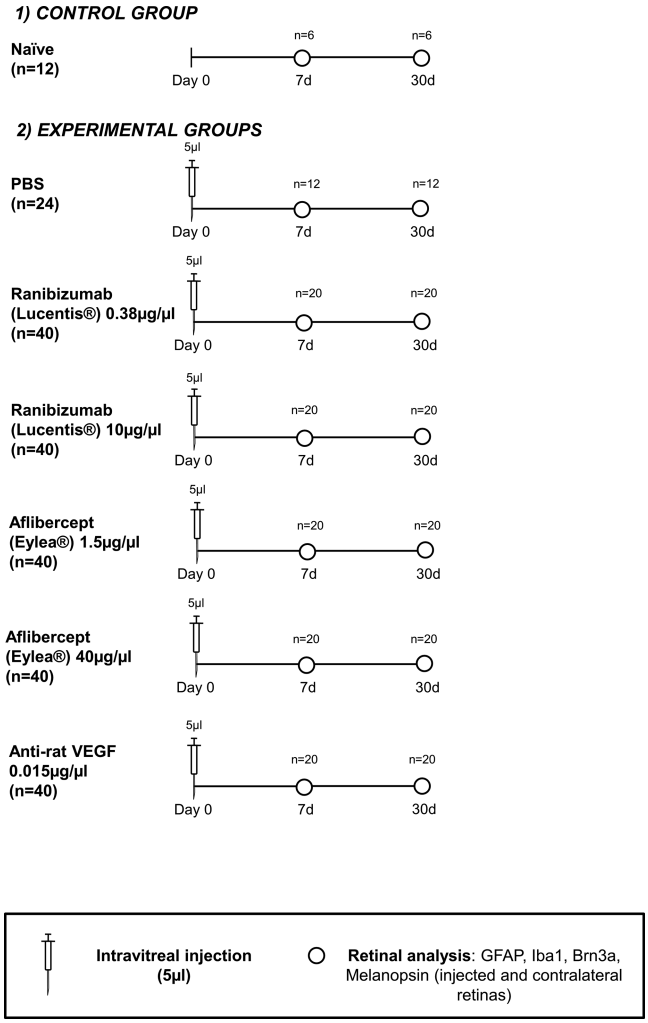

Figure 1. Experimental design. Diagram depicting the methods used: groups, substances injected, concentrations, processing times after the intravitreal injection (IVI) (days), and number of animals analyzed at each survival time (*n*).

anti-VEGF agents ranibizumab and aflibercept were used: the higher concentration that is the concentration used in clinical practice and a lower concentration diluted in PBS and calculated to obtain in the rat vitreous a concentration of the agent similar to that achieved in the human vitreous in clinical practice. To calculate the lower dose, we considered that the human vitreous had a volume of 4 mL[53] and the rat vitreous a volume of 15 µL.[54,55]

Tissue Processing

Animals were first sedated with an intraperitoneal injection of sodium pentobarbital (Dolethal Vetoquinol, S.A., Lure, France), and then euthanized with a lethal dose of sodium pentobarbital. Next, they were perfused transcardially through the ascending aorta first with saline and then with 4% paraformaldehyde in 0.1 M phosphate buffer (pH 7.4). The eyes were enucleated and the retinas were dissected as whole mounts by making four radial cuts in the superior, inferior, nasal, and temporal retinal quadrants. The cut in the superior quadrant was longer to maintain retinal orientation.[56–58] Retinas were post-fixed flat on filter paper in 4% paraformaldehyde for 1 hour, washed in PBS, and processed for immunofluorescence.

Immunohistofluorescence

Retinas were processed for immunohistofluorescence following a protocol previously described in detail by our group.[56–61] Briefly, retinas were permeabilized and incubated overnight at room temperature with a mixture of primary antibodies (see Primary Antibodies) diluted in blocking buffer (PBS containing 2% Triton X-100 and 5% normal donkey serum; Jackson ImmunoResearch, Inc., Cambridge, UK). The next morning, the retinas were incubated for 1 h at room temperature with a mixture of secondary antibodies (discussed elsewhere in this article) diluted in PBS containing 2% Triton X-100. Finally, the retinas were washed with PBS, mounted on subbed slides with the vitreous side up, and covered with an antifade mounting medium (M1289; Sigma-Aldrich).

Primary Antibodies

Two primary antibodies were used to label different populations of RGCs. The general population was labelled using a mouse anti-Brn3a antibody (1:500; mouse anti-Brn3a, MAB1585 Millipore, Madrid, Spain), and the ipRGCs were labelled with a rabbit anti-melanopsin antibody (1:500; rabbit anti-melanopsin; Invitrogen, Carlsbad, CA, USA). Microglial and macroglial (Müller cells and astrocytes) cells were labelled with rabbit anti-Iba 1 antibody (1:500; rabbit anti-Iba1; Abcam, USA, Waltham, MA, USA), goat anti-GFAP antibody (1:500; goat anti-GFAP; Abcam, USA) and goat anti-vimentin antibody (1:250, C-20, sc-7557; Santa Cruz Biotechnology, Dallas, TX, USA).

Secondary Antibodies

Goat anti-mouse IgG1 antibody Alexa Fluor 594, donkey anti-goat antibody Alexa Fluor 594, donkey anti-goat antibody Alexa Fluor 488 and donkey anti-rabbit antibody Alexa Fluor 488 were used, all diluted 1:500 (Molecular Probes, Invitrogen, Inc., Madrid, Spain).

Image Acquisition and Analysis

Retinal whole mounts were examined and photographed using a motorized Leica DM6 B fluorescence microscope (Leica, Wetzlar, Germany) equipped with various filters and magnifications (20×, 40×, or 63×, Leica Microsystems) and a Leica SP8 confocal microscope (Leica Microsystems), as previously described in detail.[52,56,62–65] Images were processed using Adobe Photoshop CS 6 (Adobe Systems, Inc., San Jose, CA, USA) when necessary.

Quantification of Brn3a$^+$ and Melanopsin$^+$ RGCs

Image-Pro Plus image analysis software (Image-Pro Plus 5.1 for Windows Media Cybernetics, Silver Spring, MD, USA) was used to quantify the total number of Brn3a$^+$RGCs using a specific macro protocol previously developed in our laboratory for the specific counting of RGC nuclei immunodetected with Brn3a in retinal whole mounts.[57,58,61,66] The obtained numerical data were exported to a spreadsheet (Microsoft

Office Excel 2003, Microsoft Corporation, Redmond, WA, USA) for further analysis. The melanopsin+RGC (ipRGC) population was quantified following a semiautomatic protocol previously described by our group.[57,65,67]

Spatial Distribution of Brn3a$^+$RGCs and ipRGCs Density Distribution

The spatial distribution of the studied populations in each retina was depicted using isodensity maps for Brn3a$^+$RGCs and neighborhood maps for ipRGCs, following previously described methods that are standard in our laboratory.[57,58,65,67,68] Both isodensity and neighborhood maps allowed the visualization of the distribution and density of these populations in a user-friendly manner, and were constructed using SigmaPlot 9.0, for Windows (Systat Software, Inc., Richmond, CA, USA).

Statistical Analyses

The GraphPad Prim software (GraphPad Prism 6, GraphPad Software, La Jolla, CA, USA) was used for statistical analysis. Numerical data are presented as mean ± SD. The data were assessed for normality and then analyzed with parametric tests. The *t* test was used for comparisons between two groups, and the one-way ANOVA (Tukey's test) or the two-way ANOVA tests were used for comparisons between several groups when one or two variables (time and different substances or concentrations used) were considered. Differences were considered significant when the *P* value was $\leq$0.05.

Results

First, we describe the glial cell reaction after the IVI with different substances and later the survival of the RGC populations studied. In each section, we first describe the findings in naïve animals, in PBS-injected animals, and in the animals that received anti-VEGF substances.

Microglial Cells

In naïve animals, microglial cells in the right and left eyes showed ramified morphology, characteristic of resting or quiescent cells, both at 7 and 30 days (Figs. 2A, 2B). In PBS-injected animals, we observed shortening of microglial cell processes and slight thickening of the soma in the left injected eyes both at 7 and 30 days after the IVI (Figs. 2C, 2I), indicating that the IVI of PBS caused a mild activation of microglial cells.

The animals that received an IVI of ranibizumab at the higher concentration (10 µg/µL) showed marked activation of microglial cells, which increased in number and had a more amoeboid form in the left retina, both at 7 and 30 days after the IVI, although these changes were more noticeable 30 days after the IVI (Figs. 2D, 2J). We could not quantify the microglial cells in this group of animals because the cells processes overlapped and thus, could not be individu-

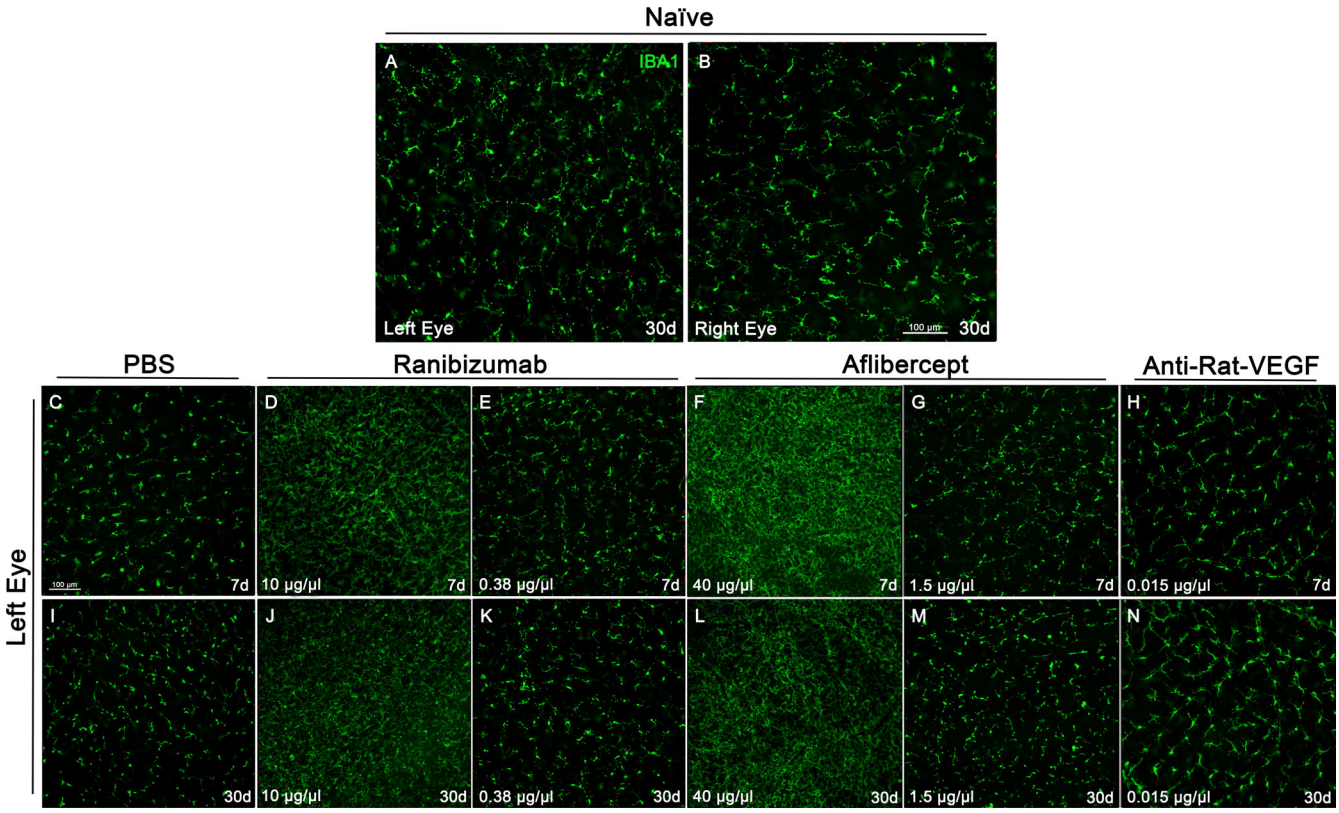

Figure 2. Microglial cell reactivity. Representative magnifications taken from the retinal flat mounts of naïve left retinas (**A**) and right retinas (**B**), and from the left retinas of the different experimental groups that received an intravitreal injection of PBS (**C**, **I**), ranibizumab 10 µg/µL (**D**, **J**) Ranibizumab 0.38 µg/µL (**E**, **K**), aflibercept 40 µg/µL (**F**, **L**), aflibercept 1.5 µg/µL (**G**, **M**) and anti-rat VEGF (**H**, **N**) showing the Iba-1$^+$ immunoreactive cells (green) at 7 (second row) and 30 (third row) days after the intravitreal injection (IVI). Scale bar, 100 µm.

Investigative Ophthalmology & Visual Science

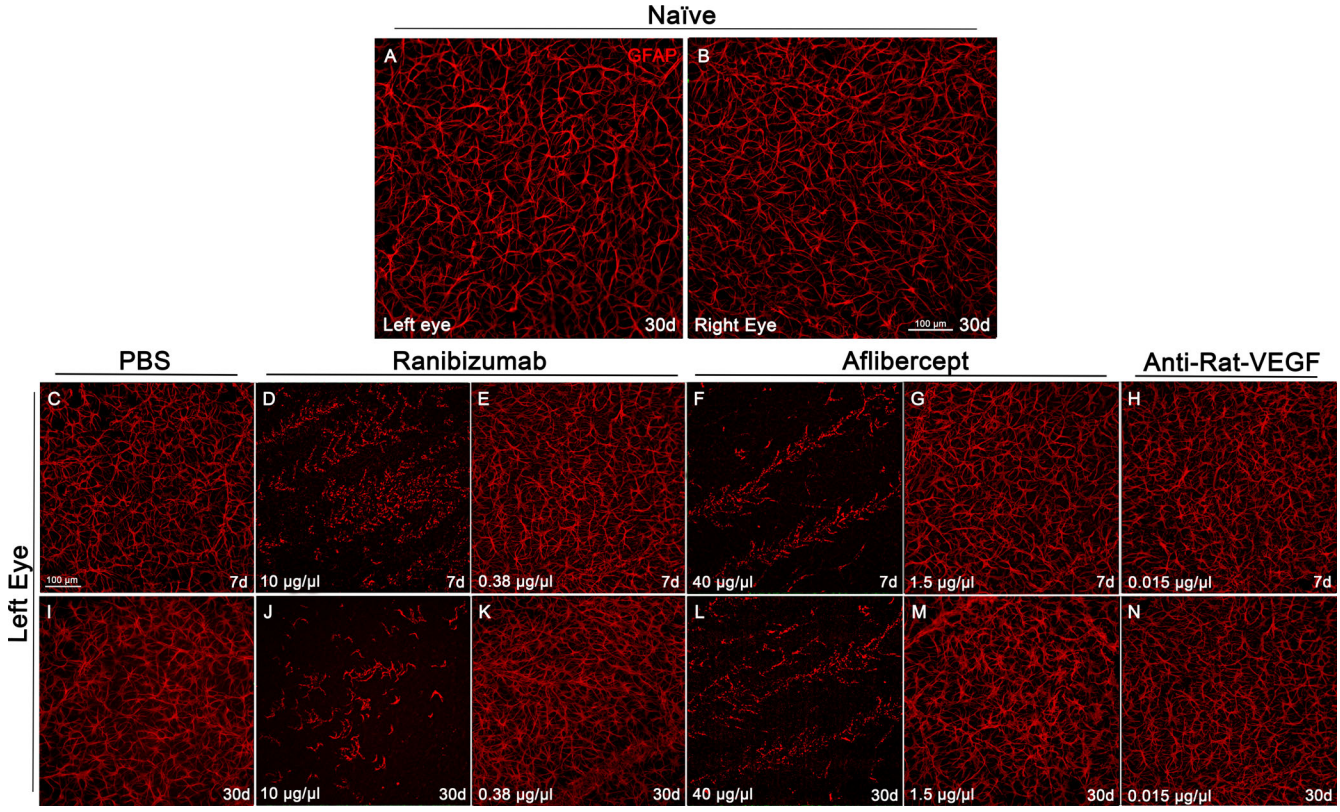

Figure 3. Macroglial cell reactivity. Representative magnifications taken from the retinal flat mounts of naïve left retinas (**A**) and right retinas (**B**), and from the left retinas of the different experimental groups that received intravitreal injections of PBS (**C**, **I**), ranibizumab 10 µg/µL (**D**, **J**), ranibizumab 0.38 µg/µL (**E**, **K**), aflibercept 40 µg/µL (**F**, **L**), aflibercept 1.5 µg/µL (**G**, **M**), and anti-rat VEGF (**H**, **N**) showing the GFAP immunoreactivity (red) at 7 days (second row) and 30 days (third row) after the intravitreal injection (IVI). Scale bar, 100 µm.

alized. The animals that received an IVI of ranibizumab at the lower concentration (0.38 µg/µL) showed some signs of microglial cell activation in the left eye: shortening of processes and more amoeboid form (Figs. 2E, 2K), similar to those found in the left eyes of the PBS group (Figs. 2C, 2I); therefore, ranibizumab at the lower concentration had a much smaller microglial reaction than at the higher concentration.

The animals that received an IVI of aflibercept at the higher concentration (40 µg/µL) showed, both at 7 and 30 days after the IVI, an increase in the number and a marked activation of microglial cells in the left eye (Figs. 2F, 2L), which resembled the microglial reaction observed in the animals that had received the higher concentration of ranibizumab (Figs. 2D, 2J). We could not quantify the number of microglial cells in these retinas because their processes overlapped. The animals that received an IVI of the lower dose of aflibercept (1.5 µg/µL), showed a much smaller microglial cell activation that resembled that found in the left eyes of the PBS group (Figs. 2G, 2M), indicating a much smaller microglial reaction with the lower dose.

The animals that received an IVI of the goat polyclonal anti-rat VEGF at the recommended dose for use in rats (0.015 µg/µL[36]) showed mild signs of microglial cell activation in the left retina: the cells had a more amoeboid shape and showed process retraction, similarly to those in the left eyes of the PBS group and in the animals that had received the lower concentration of ranibizumab or aflibercept (Figs. 2H, 2N).

In the right retinas (contralateral to the injection) of all the experimental groups, including the PBS group, we observed signs of a very subtle activation of a few microglial cells that showed a retraction of their processes (data not shown).

Macroglial Cells

The right and left retinas of the naïve animals showed a normal three-dimensional network of GFAP-labelled astrocytes in the retinal nerve fiber layer (Figs. 3A, 3B). This normal astrocyte network was observed also in the right retina of all the other groups (not shown). The animals that received a PBS injection showed slight hypertrophy of GFAP-labelled astrocytes in the left retina (Figs. 3C, 3I).[36]

The animals that received an IVI of ranibizumab or aflibercept at the higher concentration (10 µg/µL or 40 µg/µL, respectively) showed an important change in GFAP expression in the injected left retinas. There were arrow-shaped areas of increased GFAP immunoreactivity both 7 and 30 days after IVI (Figs. 3D, 3F, 3J, 3L) that were also vimentin immunoreactive and thus correspond to the end feet of Müller cells (Fig. 4). The astrocyte cell bodies could not be individualized in the areas of higher GFAP expression because they were obscured by the higher immunoreactivity, but could be seen outside these areas (Fig. 4). The animals that received an IVI of the lower concentration of ranibizumab or aflibercept (0.38 µg/µL and 1.5 µg/µL, respectively) showed in the left retinas only a slight hyper-

Investigative Ophthalmology & Visual Science

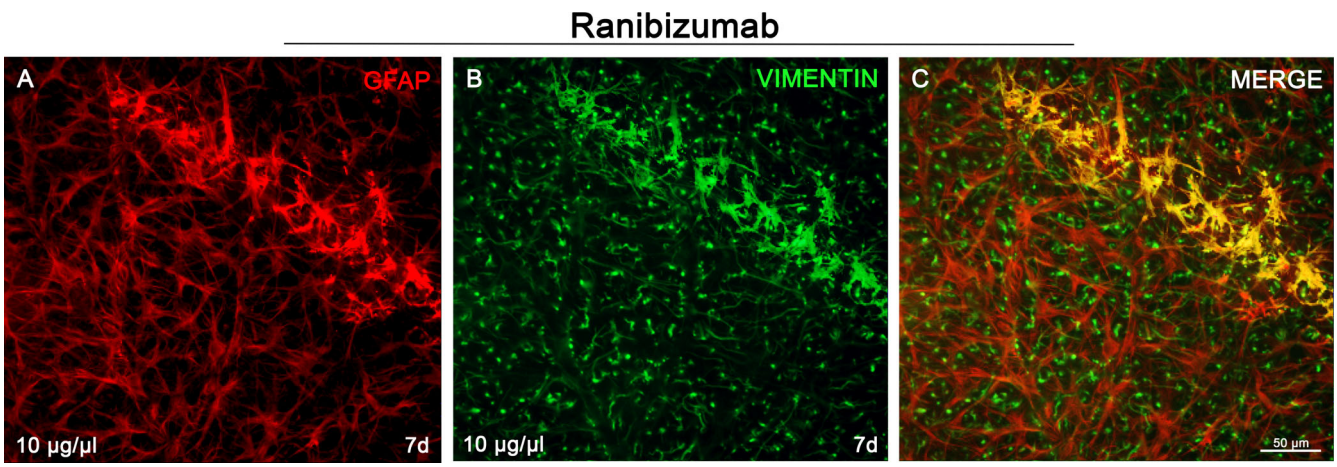

Figure 4. Confocal photomicrographs of the same retinal area of a left retina of one animal that had received an intravitreal injection (IVI) of ranibizumab at the 10-µg/µL concentration and was processed 7 days later. The micrographs were taken with different fluorescence filters to show the glial fibrillary acidic protein (GFAP) immunoreactivity (**A**), the vimentin immunoreactivity (**B**), or a merged image (**C**). GFAP and vimentin immunoreactivity colocalize in the hyperfluorescent areas of the inner retinal surface, indicating that they correspond to the end feet of Müller cells. Scale bar, 50 µm.

trophy of the astrocytes (Figs. 3E, 3G, 3K, 3M), similar to that found in the left eyes of the PBS-injected animals (Figs. 3C, 3I). The animals that had received IVI of the polyclonal anti-rat VEGF antibody showed in the left retinas a slight thickening and shortening of the astrocyte processes (Figs. 3H, 3N), similar to that found in PBS-injected animals and in animals that had received the lower dose of ranibizumab and aflibercept.

RGC Survival

In naïve animals, the mean number ± SD of Brn3a$^+$RGCs per retina (81,022 ± 3883; $n = 6$) (Fig. 5O; Table) was similar to that reported in previous studies by our group.[57,61] In the PBS group (Figs. 5C, 5I, 5O), the numbers of Brn3a$^+$RGCs in the left (injected) retinas at 7 days (81,175 ± 942; $n = 6$) and 30 days (80,935 ± 2325; $n = 6$) after the IVI were similar to those found in the retinas of naïve animals and in the right (uninjected) retinas of the same group at 7 days (80,117 ± 2158; $n = 10$) and 30 days (80,900 ± 2100; $n = 10$) after the IVI. Thus, the IVI of PBS had no effect on Brn3a$^+$RGCs survival during the first month after the IVI (Table).

In the animals that received ranibizumab at the higher concentration, the mean numbers of Brn3a$^+$RGCs in the left (injected) eyes were 71,947 ± 2889 ($n = 10$) at 7 days and 71,135 ± 3866 ($n = 10$) at 30 days (Figs. 5D, 5J, 5O; Table), whereas the mean numbers of Brn3a$^+$RGCs in the contralateral right eyes were 79,214 ± 2508 ($n = 10$) and 78,152 ± 3028 ($n = 10$) at 7 and 30 days after the IVI, respectively. The numbers found in the right retinas of this group were similar to those observed in the left and right retinas of the naïve and PBS groups (Figs. 5B, 5O), but the numbers found in the left retinas were significantly smaller than those found in the right retinas ($P < 0.001$) and represented a decrease of 11% and 12% of the Brn3a$^+$RGC population at 7 and 30 days after the IVI, respectively (Fig. 5O; Table). However, there were no significant differences between the numbers of Brn3a$^+$RGCs found in the left retinas of this group 7 and 30 days after the IVI (Table).

In the animals that received the lower concentration of ranibizumab, the mean numbers of Brn3a$^+$RGCs in the left (injected) retinas were 78,530 ± 4240 ($n = 10$) and 78,914 ± 4900 ($n = 10$) 7 and 30 days after the IVI and in the right uninjected eyes 76,822 ± 2959 ($n = 10$) and 78,974 ± 4911 ($n = 10$) at 7 and 30 days after the IVI, respectively (Table). The numbers of Brn3a$^+$RGCs were similar between the left and right retinas and comparable to the numbers found in the retinas of naïve and PBS animals (Figs. 5E, 5K, 5O; Table).

The animals that received aflibercept at the higher concentration had mean numbers of Brn3a$^+$RGCs in the left (injected) eyes of 73,533 ± 2096 ($n = 10$) and 71,523 ± 3171 ($n = 10$) at 7 and 30 days after the IVI, respectively (Figs. 5F, 5L, 5O), and in the uninjected right eye of 81538 ± 1,314 ($n = 10$) and 80579 ± 1,519 ($n = 10$) 7 and 30 days after IVI, respectively. The numbers found in the right retinas of this group were similar to those found in the retinas of naïve and PBS-injected animals (Figs. 5B, 5O; Table). The numbers found in the left retinas were significantly smaller than those found in the right retinas ($P < 0.001$) both 7 and 30 days after the IVI (Fig. 5O; Table) and represented a loss of 9.8% and 11.0% of the Brn3a$^+$RGC population, respectively. However, there were no significant differences between the numbers found in the left retinas at days 7 and 30 after the IVI.

In the animals that received aflibercept at the lower dose, the mean number of Brn3a$^+$RGCs in the left eye was 76,916 ± 5666 ($n = 10$) and 79,454 ± 4420 ($n = 10$) at 7 and 30 days after the IVI, respectively (Figs. 5G, 5M, 5O), and the mean numbers found in the right (uninjected) eyes were 77,678 ± 5179 ($n = 10$) and 79,504 ± 5058 ($n = 10$) at 7 and 30 days after the IVI, respectively (Figs. 5B, 5O; Table). In this group, there were no statistically significant differences between the right and left eyes at any of the time points studied and thus, we could not document RGC loss (Fig. 5O; Table).

The animals that received an IVI of the polyclonal anti-rat VEGF antibody had numbers of Brn3a$^+$RGCs in the left eye of 80,375 ± 1369 ($n = 10$) and 80,083 ± 1041 ($n = 10$), 7 and 30 days after the IVI, respectively (Figs. 5G, 5M, 5O; Table). These animals had numbers of Brn3a$^+$RGCs in the right (uninjected) eyes of 80,231 ± 833 ($n = 10$) and 81,519 ± 1798 ($n = 10$) at 7 and 30 days after the IVI, respectively (Figs. 5B, 5O; Table). There were no statistically significant differences between the numbers found in the left and right

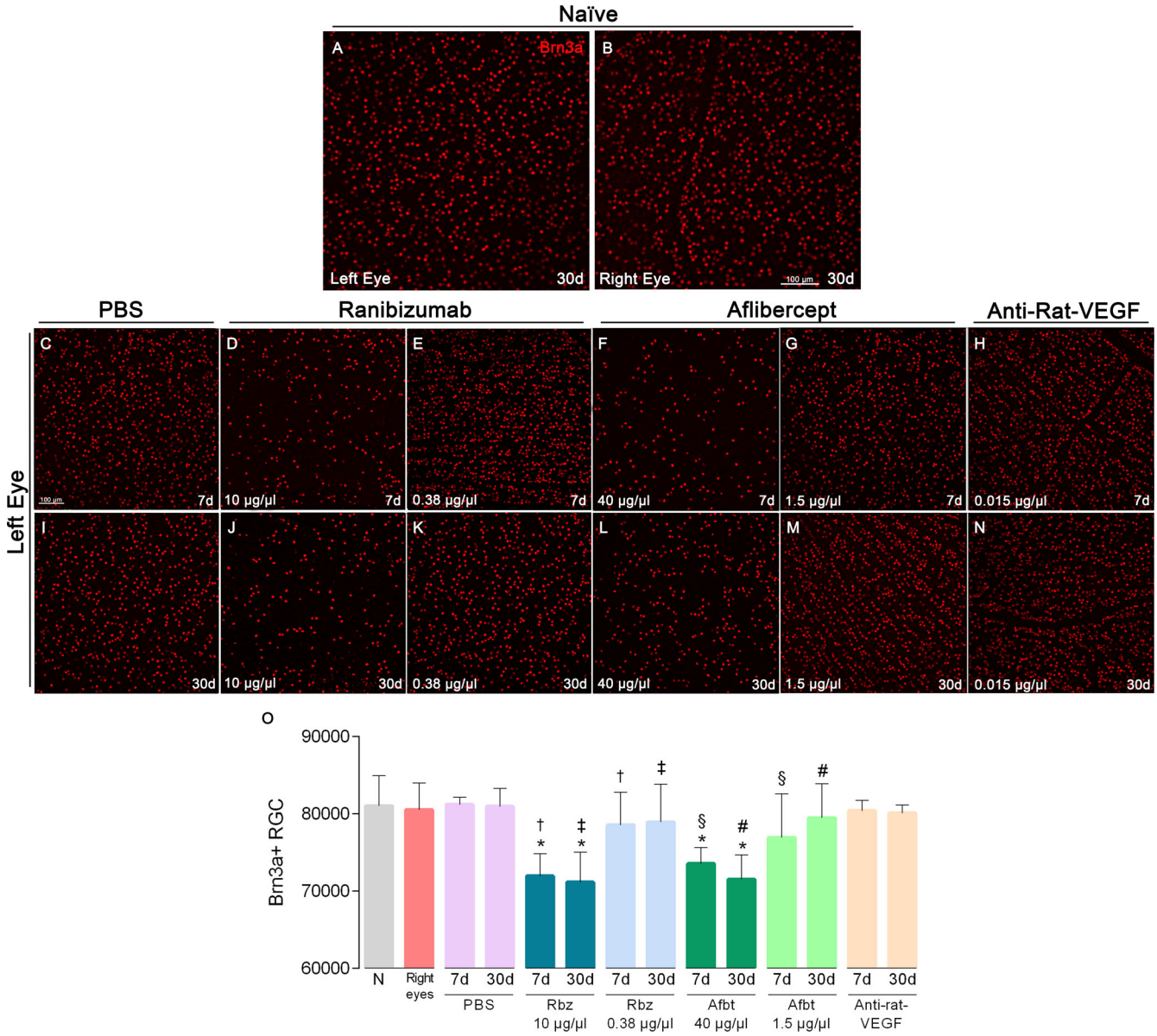

Figure 5. Brn3a$^{\pm}$RGC survival. Representative magnifications taken from the retinal flat mounts of the naïve left retinas (**A**) and right retinas (**B**), and from the left retinas of the different experimental groups that received an intravitreal injection of PBS (**C**, **I**), ranibizumab 10 µg/µL (**D**, **J**), ranibizumab 0.38 µg/µL (**E**, **K**), aflibercept 40 µg/µL (**F**, **L**), aflibercept 1.5 µg/µL (**G**, **M**), and anti-rat VEGF (**H**, **N**), showing Brn3a^{+} cells (red) at 7 days (second row) and 30 days (third row) after the intravitreal injection (IVI). Scale bar, 100 µm. (**O**) Bar graph showing mean numbers ± SD of Brn3a^{+}RGCs per retina in naïve animals (N, grey; $n = 3$ animals: 6 retinas, 3 left retinas and 3 right retinas), right retinas of the experimental animals (right eyes, red; $n = 106$ retinas), and left retinas of eyes of experimental animals that received IVI of PBS (purple; $n = 6$ at each survival time), ranibizumab 10 µg/µL (Rbz, dark blue; $n = 10$ at each survival time), ranibizumab 0.38 µg/µL (Rbz, light blue; $n = 10$ at each survival time), aflibercept 40 µg/µL (Afbt, dark green; $n = 10$ at each survival time), aflibercept 1.5 µg/µL (Afbt, light green; $n = 10$ at each survival time), and anti-rat VEGF (orange; $n = 10$ at each survival time). *Statistically significant differences between the left injected retinas and the naïve eyes, the right eyes, and the other experimental groups at the same survival time ($P \leq 0.0001$; one-way- ANOVA, Tukey's test). † Statistically significant difference with the lower dose of the same substance (ranibizumab) at 7 days ($P \leq 0.0001$; t test). ‡Statistically significant difference with the lower dose of the same substance (ranibizumab) at 30 days ($P \leq 0.0001$; t test). § Statistically significant difference with the lower dose of the same substance (aflibercept) at 7 days ($P = 0.0018$; t test). # Statistically significant difference with the lower dose of the same substance (aflibercept) at 30 days ($P \leq 0.0001$; t test).

retinas of this group of animals or between the numbers found in this group and the numbers found in the retinas of the naïve and PBS groups (Fig. 5O; Table).

We also compared the mean numbers of Brn3a^{+}RGCs in the left eye between the different experimental groups and found that the groups that showed significant decreases in RGCs numbers were those that received ranibizumab or aflibercept at the higher concentration when compared with naïve animals, both 7 days ($P < 0.001$ and $P = 0.02$, respectively) and 30 days ($P < 0.001$) after the IVI (Fig. 5O; Table). However, no significant difference was found between the numbers of Brn3a^{+}RGCs in the left eyes of animals that received the IVI of ranibizumab or aflibercept at the lower concentration and the naïve animals (Table). Finally, both in

Table.

	Brn3a$^+$RGCs	Melanopsin$^+$ RGCs
Naive		
7 days	81,021 ± 3883	2190 ± 138
30 days	80,954 ± 3657	2124 ± 119
Right eyes		
7 days	80,505 ± 3482	2190 ± 138
30 days	81,684 ± 3278	2098 ± 109
PBS		
7 days	81,175 ± 942	2155 ± 159
30 days	80,934 ± 2325	2150 ± 334
Ranibizumab (10 µg/µl)		
7 days	71,947 ± 2889[*,†]	1977 ± 251
30 days	71,134 ± 3866[*,‡]	2154 ± 211
Ranibizumab (0.38 µg/µl)		
7 days	78,530 ± 4240[†]	2078 ± 175
30 days	78,913 ± 4899[‡]	2199 ± 133
Aflibercept (40 µg/µl)		
7 days	73,533 ± 2096[*,§]	2168 ± 101
30 days	71,523 ± 3171[*,#]	2153 ± 336
Aflibercept (1.5 µg/µl)		
7 days	76,916 ± 5666[§]	2021 ± 334
30 days	79,453 ± 4420[#]	2119 ± 110
Anti-rat-VEGF		
7 days	80,375 ± 1369	2117 ± 102
30 days	80,083 ± 1041	2036 ± 107

Mean numbers (±SD) of Brn3a+ and melanopsin+RGCs per retina in the different groups at different survival times.

[*] Statistically significant differences between the Naïve, Right eye, and other experimental groups at the same time point ($P \leq 0.0001$; One Way-ANOVA, Tukey's test).

[†] Statistically significant differences with the animals that received the same substance (ranibizumab) at a lower dose at 7 days ($P \leq 0.0001$; *t*-test).

[‡] Statistically significant differences with the lower dose of the same substance (ranibizumab) at the same time point ($P \leq 0.0001$; *t*-test).

[§] Statistically significant differences with the lower dose of the same substance (ranibizumab) at 30 days ($P = 0.0018$; *t*-test).

[#] Statistically significant differences with the lower dose of the same substance (aflibercept) at 7 days ($P \leq 0.0001$; *t*-test).

the ranibizumab and in the aflibercept groups, there were significantly lower numbers of Brn3a$^+$ RGCs in the left eyes that had received the higher concentration than in the left eyes that had received the lower concentration (Fig. 5O; Table).

RGC Distribution

In naïve animals, the Brn3a$^+$RGC isodensity maps showed a higher density of RGCs in the superotemporal region of the retina (Figs. 6A, 6B), as described previously by our group.[57,58,65] In PBS-injected animals, the spatial distribution of Brn3a+RGCs was similar to that observed in the naïve group (Figs. 6C, 6I). The groups that received ranibizumab or aflibercept at the higher concentration showed a diffuse decrease of the warm colors in the left (injected) eyes at 7 and 30 days after the IVI indicating RGC loss (Figs. 6D, 6F, 6J, 6L). However, the animals that received an IVI of ranibizumab or aflibercept at the lower concentration and the animals that received an IVI of the rat-specific anti-VEGF showed in the left and right eyes RGC isodensity maps similar to those of naïve and PBS-injected animals (Figs. 6E, 6G, 6H, 6K, 6M, 6N).

ipRGC Survival

ipRGC Numbers. In naïve animals, the mean numbers of ipRGCs in the retinas (2190 ± 138; $n = 6$) (Figs. 7A, 7B, 7O; Table) were similar to that reported in previous studies by our group[57,67] and to that found in the retinas of PBS-injected animals (2,155 ± 333; $n = 6$) (Figs. 7C, 7I, 7O; Table).

The groups that received the IVI of ranibizumab, aflibercept or polyclonal anti-rat VEGF, also showed similar mean numbers of ipRGCs in the left retinas, irrespective of the substance or dose used (Fig. 7O; Table). The mean numbers of ipRGCs in the left retina of the animals that received ranibizumab or aflibercept at the higher concentration were 2154 ± 211 and 2153 ± 335, respectively, at 7 days, and 2078 ± 175 and 2021 ± 336, respectively, at 30 days after the injection (Table). In the animals that received ranibizumab or aflibercept at the lower concentration these numbers were 2199 ± 133 and 2120 ± 110, respectively, at 7 days, and 2168 ± 101 and 2117 ± 102, respectively, at 30 days after the injection (Table). The animals that received an IVI of the polyclonal anti-rat VEGF antibody had numbers of ipRGCs in the left retina of 2036 ± 117and 1825 ± 232 at 7 and 30 days after the injection, respectively. These numbers were similar to those found in naïve and PBS-injected animals (Figs. 7D–7H, 7J–7N; Table). See Supplementary Figure S1 for ipRGCs distribution.

ipRGC Distribution. The spatial distribution of ipRGCs in neighborhood maps was in naïve animals similar to that found in previous studies of our group[57,65,67] (Supplementary Figs. S1A, S1B), with a higher density of ipRGCs in the superotemporal region of the retina. This distribution did not change in the left and right eyes of the animals that received PBS or anti-VEGF substances and was thus similar to the observed naïve animals (Supplementary Figs. S1C–S1N).

Discussion

In this study, we analyzed the effects of a single IVI of two different concentrations of two of the most commonly used humanized anti-VEGF drugs in clinical practice: the monoclonal antibody ranibizumab and the fusion protein aflibercept, as well as a rat-specific monoclonal anti-VEGF antibody, in the rat retina. We have used two different concentrations of the anti-VEGF substances (the one used in humans and a lower concentration calculated for the rat eye) because, in previous published studies, the humanized anti-VEGF had been used in rats at the concentrations used in clinical practice[69–71] and also because, in a previous study, we had observed a marked glial cell reaction in the rat retina after single and multiple IVIs of bevacizumab at the concentration used in humans.[36] Therefore, in this study, we aimed to analyze the interspecies immunological tolerance and responses to the two most commonly used drugs in clinical practice, ranibizumab and aflibercept. We have analyzed glial reactivity and RGC survival and whether they were concentration and/or substance dependent.

Animals injected with PBS exhibited microglial cell activation in the left-injected retina, as indicated by the retraction of microglial cell processes and a more amoeboid shape. Microglial cells are first responders to retinal insults[62,72,73] and play a crucial role in mediating inflammatory responses and maintaining retinal homeostasis.[51,56,62,63,74–76] We did not quantify the microglial cells in these retinas because

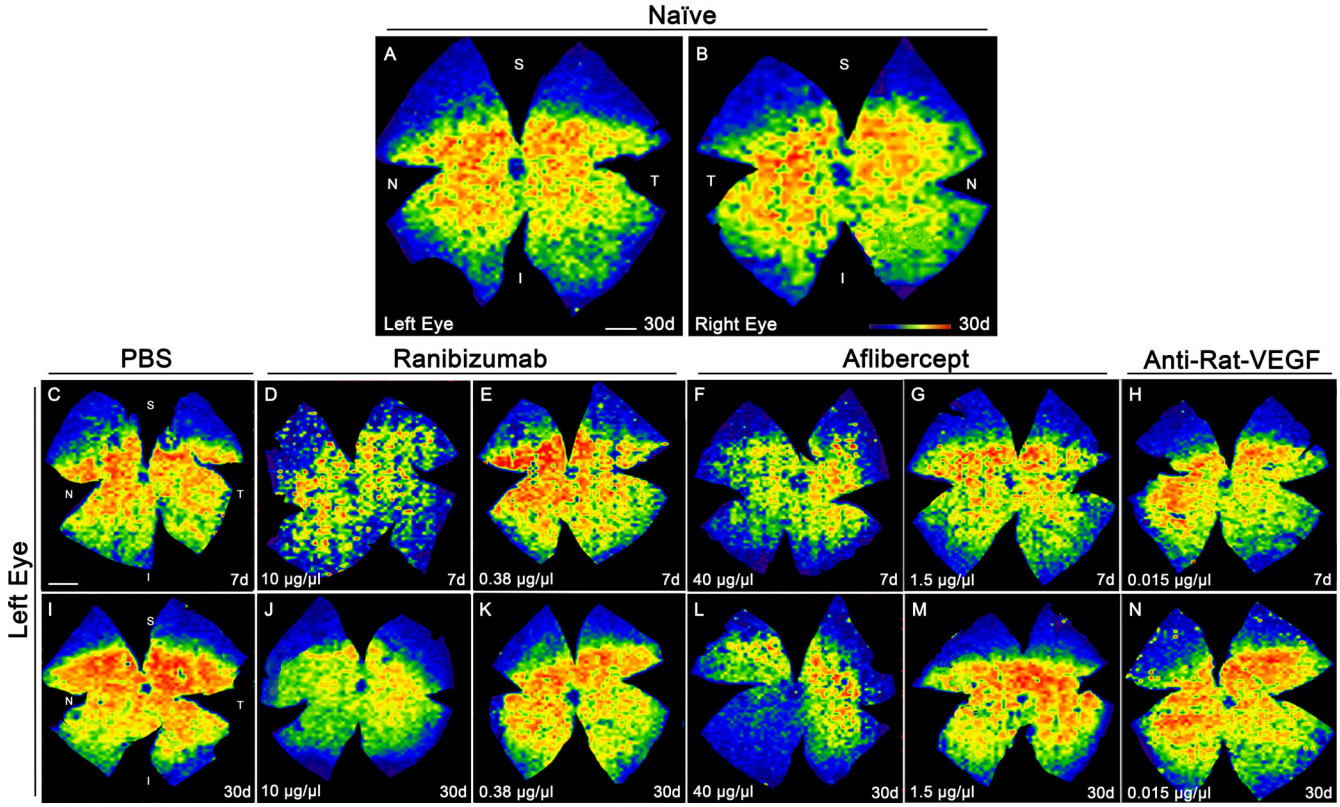

Figure 6. Topography of Brn3a$^{\pm}$RGC after intravitreal injection (IVI) of different anti-VEGF agents. Representative isodensity maps showing the topography of Brn3a^{+}RGC in naïve left retinas (**A**) and right retinas (**B**), and the left retinas of the experimental groups that received an intravitreal injection of PBS (**C**, **I**), ranibizumab 10 µg/µL (**D**, **J**), ranibizumab 0.38 µg/µL (**E**, **K**), aflibercept 40 µg/µL (**F**, **L**), aflibercept 1.5 µg/µL (**G**, **M**), and anti-rat VEGF (**H**, **N**). The color scale bar at the bottom of (**B**) indicates cell density from 0 (purple) to ‡3500 (red). Scale bar, 100 µm.

we had previously documented that in the rat the IVI of PBS causes an increase in microglial cell density.[36] In the right eye, a subtle activation of some microglial cells was observed after PBS injection in the left eye (data not shown), which is consistent with the results of a previous study by our group.[36]

Animals that received an IVI of ranibizumab and aflibercept also exhibited a microglial cell reaction in the left eye, but its degree differed depending on the administered concentration. Injection of the lower concentration, calculated to obtain in the rat eye the same concentration as in the human eye in clinical practice, resulted in a slight activation of microglial cells, similar to that observed in the left eye of the PBS-injected animals. In contrast, injection of the higher concentration, the dose used in human clinical practice, led to a more pronounced microglial cell reaction, characterized by increased microglial cell numbers in the left retinas that could not be quantified because of their overlapping processes. Ranibizumab is the truncated form of bevacizumab, a humanized monoclonal antibody,[77] and aflibercept is an RNA trap, a fusion protein that contains portions of the extracellular domains 1 and 2 of the human VEGF receptor.[77] Therefore, both could cause an immunological response in rats. We document that the lower concentration causes a mild microglial cell activation, but that the higher concentration elicits a strong microglial cell reaction, similar to that observed by our group previously with the IVI of bevacizumab at the human clinical concentration.[36]

The IVI of the polyclonal anti-rat VEGF antibody also resulted in a minor microglial cell reaction in the left retina, resembling the response observed in PBS-injected animals and in those injected with the lower concentration of ranibizumab and aflibercept. Thus, in all the left-injected eyes we have documented a mild activation of microglial cells throughout the retina, evidenced by a transition from their typical branched morphology to an amoeboid shape, accompanied by shortening of their processes. This finding is in accordance with previous studies showing in the rat retina microglial activation following IVI of humanized anti-VEGF or other substances.[36,48,78,79] This activation was in this study influenced by the concentration of the anti-VEGF substance employed, because it was more pronounced with the higher concentrations. In the retinas injected with the higher concentration it was not possible to quantify the numbers of microglial cells because their processes overlapped and therefore we cannot document increased densities of microglial cells. Our results are in contrast with those of another study that reported a decrease in microglial cell activation following IVI of ranibizumab at the higher concentration used in our study in a rat ischemia–reperfusion model.[80] However, the same study showed an increase in microglial activation after IVI of bevacizumab.[80] In human patients, there is an ongoing debate regarding the role of anti-VEGF in ocular inflammation because ranibizumab or aflibercept could decrease inflammatory factors (i.e., cytokines) related to microglial activation.[81–85] However, whether the decreased cytokine levels result from VEGF

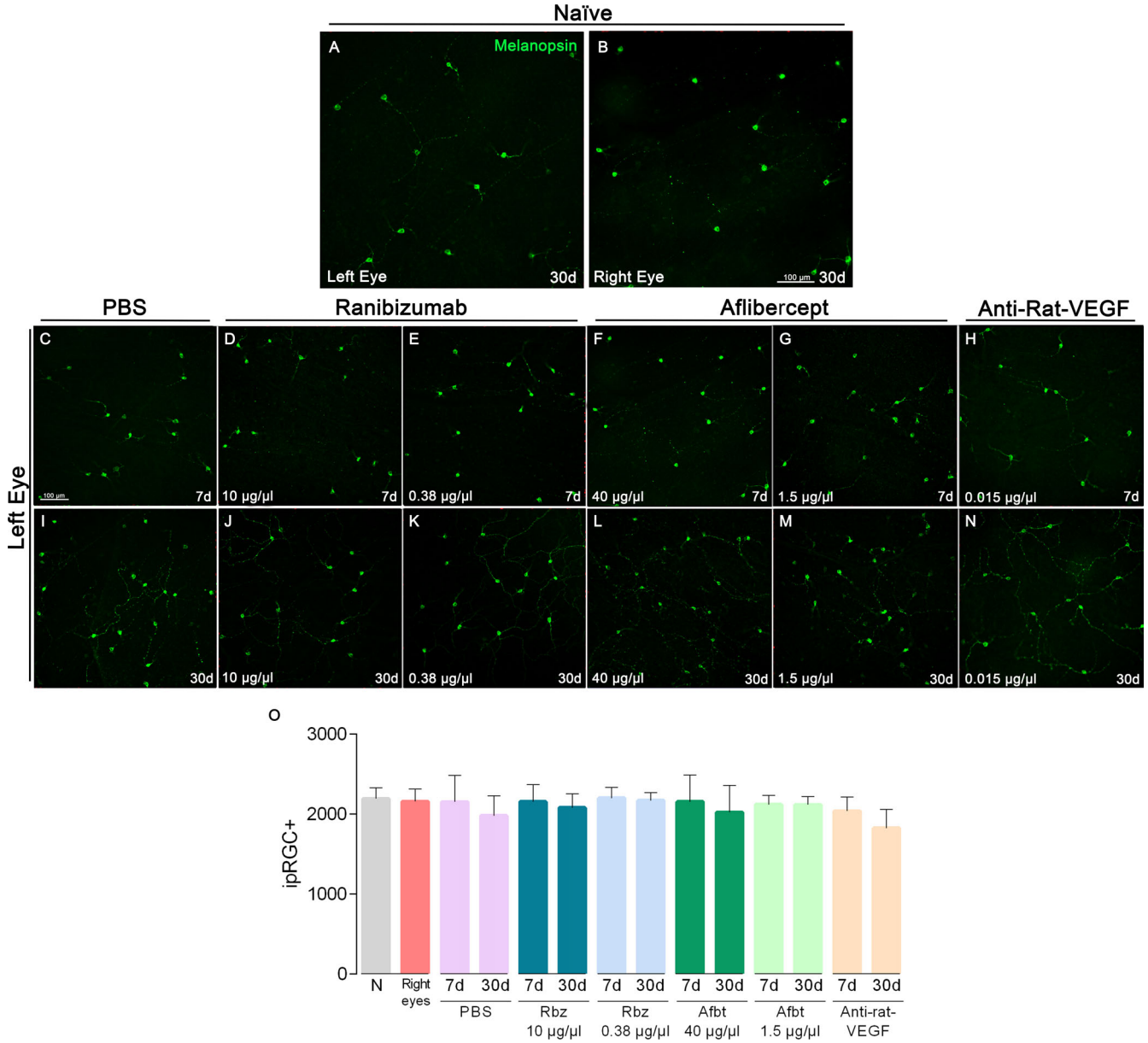

Figure 7. Intrinsically photosensitive retinal ganglion cell (ipRGC) survival. Representative magnifications taken from retinal flat mounts of naïve: left eyes (**A**) and right eyes (**B**), and the different experimental groups that received an intravitreal injection of PBS (**C**, **I**), ranibizumab 10 µg/µL (**D**, **J**), ranibizumab 0.38 µg/µL (**E**, **K**), aflibercept 40 µg/µL (**F**, **L**), aflibercept 1.5 µg/µL (**G**, **M**), and anti-rat VEGF (**H**, **N**) showing IpRGC^{+} cells (green). Scale bar, 100 µm. (**O**) Bar graphs showing mean ± SD of Brn3a^{+}RGCs in naïve animals (N, grey; $n = 3$ animals: 6 retinas, 3 left retinas and 3 right retinas). Right retinas of the experimental animals (right eyes, red; $n = 106$ retinas), and left retinas of experimental animals that received intravitreal injection (IVI) of PBS (purple; $n = 6$ at each survival time), ranibizumab 10 µg/µL (Rbz, dark blue; $n = 10$ at each survival time), ranibizumab 0.38 µg/µL (Rbz, light blue; $n = 10$ at each survival time), aflibercept 40 µg/µL (Afbt, dark green; $n = 10$ at each survival time), aflibercept 1.5 µg/µL (Afbt, light green; $n = 10$ at each survival time), and anti-rat VEGF (Orange; $n = 10$ at each survival time). There were no significant differences between the groups.

signaling suppression or are an indirect consequence of decreased vascular disease remains unclear.[7] Indeed, it has been documented that patients affected by retinal diseases who do not respond to ranibizumab show increased levels of proinflammatory factors.[86]

We also observed astrocyte hypertrophy and marked GFAP overexpression in the rat retina after IVI. Astrocyte hypertrophy was observed in the left eyes of PBS-injected animals and those injected with the lower dose of ranibizumab or aflibercept, whereas areas of marked GFAP immunoreactivity were observed in the inner surface of the retina in the animals injected with ranibizumab or aflibercept at the higher dose. These areas exhibited distinct curved arrow-shaped patterns, which we document here and we have shown previously, using double labeling with vimentin that is specific for Müller cells that correspond with GFAP upregulation in Müller cell peduncles.[36] Within these areas of increased GFAP immunoreactivity, the normal network of astrocytes cannot be seen, but previous studies of our laboratory and other groups have shown the persistence

of the macroglial cell network in these areas.[36,78] Our findings are in agreement with previous studies showing that the IVI elicit astrocyte hypertrophy and Müller cell hyperreactivity, and that the substance injected influences their extent.[36,45,48,78,87] Finally, although in vitro studies using ocular cell lines from different species for toxicology testing (ARPE19 cells and 661W cells) have suggested minimal toxicity for aflibercept, ranibizumab, and bevacizumab,[88] other studies have demonstrated that these substances cause metabolic and molecular changes in human Müller cells in vitro[41,42] and GFAP overexpression in rabbits[43] and rats primary retinal cultures.[44] Glial cells are the first cells to react to an insult or stress in the retina,[51,56,58,62,74,76,89,90] and their activation is, therefore, a good indicator of drug- or treatment-induced retinal changes.

We have also studied the impact of IVI on the survival of the general population of RGCs and the ipRGCs. The higher dose of ranibizumab and aflibercept resulted in RGC loss in rats at the time points examined. This finding suggests that the above-mentioned glial reaction that occurs after IVI of humanized anti-VEGF in rats[36] can result in RGC death. However, the contrary is also possible, that this reaction may be due to a direct toxic effect of the anti-VEGF substances on RGCs. Our findings contradict, however, previous research that reported that the IVI of pegaptanib, ranibizumab, and bevacizumab in rats had no toxic effects on the retina and did not affect RGC survival.[46,47,49] Furthermore, our results support those of another study that documented apoptosis in the ganglion cell layer following IVI of anti-VEGF antibody in diabetic rats.[91] The IVIs of humanized aflibercept, bevacizumab, and ranibizumab have also been reported to induce apoptosis in various retinal layers of the rabbit retina.[92] Consistent with our results, a recent study has shown that the IVI of ranibizumab causes dose-dependent apoptotic RGC death in the rat retina[37] and that repeated IVIs further increased RGC apoptosis.[37] In this study, we document that approximately one-eighth of the general RGC population was lost in the first 7 days after the injection of ranibizumab or aflibercept at the higher dose. However, we do not know whether this diffuse RGC loss has an impact in visual function.

Finally, we found that the IVI of ranibizumab or aflibercept, even at higher concentrations, did not affect the number of ipRGCs at the doses administered, suggesting that the ipRGCs may be more resistant to the toxic effects of the anti VEGF factors or to inflammation than the general population of RGCs. This resilience of the ipRGCs to different noxious stimuli has been demonstrated in various pathological and experimental conditions.[57,65,93–97]

This study has some limitations. For example, PBS was used as a diluting agent and it would have been more correct to use an isotype control antibody. Thus, we cannot ascertain if the results observed are due to anti-VEGF binding in an antigen-specific manner or to non–antigen-specific binding or other nonspecific interactions. Another limitation is that we have not carried out repeated injections, which would better simulate clinical practice. Thus, it is possible that the loss of RGCs could be greater after multiple injections, but we cannot confirm it. Last, another limitation of our model might be that we have used healthy animals. Although the primary objective of the study was to examine the potential deleterious consequences of these injections on the healthy retina, we could have used animals with photoreceptor degenerations or resembling age related macular degeneration to better match the clinical practice. Because AMD is a degenerative disease characterized by inflammation,[98] it is possible that the anti-VEGF injections may increase retinal inflammation, but many clinical studies have documented that their beneficial effects in the neovascular form prevail over their possible adverse effects.[16,86,98,99]

In summary, our findings reveal in the rat retina, microglial activation, and astrocyte hypertrophy after IVI of different substances, even after PBS injection, and a stronger microglial and macroglial cell response after IVI of ranibizumab and aflibercept at the higher concentration that is accompanied of RGCs death but not ipRGC death. It remains to be shown whether this RGC death is a direct toxic effect of the humanized ranibizumab or aflibercept on RGCs or an indirect effect, consequence of glial cell activation in the retina triggered by an immunological response. Therefore, our results highlight the potential inflammatory and death-promoting effects of the interspecies use of anti-VEGF agents at high doses, and also the resilience of the ipRGCs.

Acknowledgments

Funding provided by the Instituto de Salud Carlos III (ISCIII): PI19/00203, co-funded by ERDF, "A way to make Europe" to MPV-P and DG-A, and PI22/00900, co-funded by the European Union, to MPV-P and DG-A, and RD16/0008/0026 co-funded by ERDF, "A way to make Europe" to MPV-P and RD21/0002/0014 financiado por la Unión Europea – NextGenerationEU; RED2018-102499-T and PID2019-106498GB-I00 funded by MCIN/AEI/=10.13039/501100011033 to MV-S.

Disclosure: **A. Martínez-Vacas**, None; **J. Di Pierdomenico**, None; **A.M. Gómez-Ramirez**, None; **M. Vidal-Sanz**, None; **M.P. Villegas-Pérez**, None; **D. García-Ayuso**, None

References

1. Tolentino M. Systemic and ocular safety of intravitreal anti-VEGF therapies for ocular neovascular disease. *Surv Ophthalmol*. 2011;56:95–113.
2. Bernatchez PN, Soker S, Sirois MG. Vascular endothelial growth factor effect on endothelial cell proliferation, migration, and platelet-activating factor synthesis is Flk-1-dependent. *J Biol Chem*. 1999;274:31047–31054.
3. Pozarowska D, Pozarowski P. The era of anti-vascular endothelial growth factor (VEGF) drugs in ophthalmology, VEGF and anti-VEGF therapy. *Cent Eur J Immunol*. 2016;41:311–316.
4. Liu ZL, Chen HH, Zheng LL, Sun LP, Shi L. Angiogenic signaling pathways and anti-angiogenic therapy for cancer. *Signal Transduct Target Ther*. 2023;8:198.
5. Barleon B, Sozzani S, Zhou D, Weich HA, Mantovani A, Marme D. Migration of human monocytes in response to vascular endothelial growth factor (VEGF) is mediated via the VEGF receptor flt-1. *Blood*. 1996;87:3336–3343.
6. Reinders ME, Sho M, Izawa A, et al. Proinflammatory functions of vascular endothelial growth factor in alloimmunity. *J Clin Invest*. 2003;112:1655–1665.
7. Uemura A, Fruttiger M, D'Amore PA, et al. VEGFR1 signaling in retinal angiogenesis and microinflammation. *Prog Retin Eye Res*. 2021;84:100954.
8. Shibuya M. Vascular endothelial growth factor (VEGF) and its receptor (VEGFR) signaling in angiogenesis: a crucial

target for anti- and pro-angiogenic therapies. *Genes Cancer*. 2011;2:1097–1105.
9. GBD 2019 Blindness and Vision Impairment Collaborators; Vision Loss Expert Group of the Global Burden of Disease Study. Trends in prevalence of blindness and distance and near vision impairment over 30 years: an analysis for the Global Burden of Disease Study. *Lancet Glob Health*. 2021;9:e130–e143.
10. European public assessment report. European Medicines Agency. Science Medicines Health, http://www.ema.europa.eu/.
11. U.S. FOOD & DRUG ADMINISTRATION, New Hampshire, https://www.fda.gov/.
12. Ferrara N. Vascular endothelial growth factor as a target for anticancer therapy. *Oncologist*. 2004;9(Suppl 1):2–10.
13. Gragoudas ES, Adamis AP, Cunningham ET, Jr., Feinsod M, Guyer DR, Group VISiONCT. Pegaptanib for neovascular age-related macular degeneration. *N Engl J Med*. 2004;351:2805–2816.
14. Sivaprasad S. Role of pegaptanib sodium in the treatment of neovascular age-related macular degeneration. *Clin Ophthalmol*. 2008;2:339–346.
15. Brown DM, Michels M, Kaiser PK, et al. Ranibizumab versus verteporfin photodynamic therapy for neovascular age-related macular degeneration: two-year results of the ANCHOR study. *Ophthalmology*. 2009;116:57–65.e55.
16. Rosenfeld PJ, Brown DM, Heier JS, et al. Ranibizumab for neovascular age-related macular degeneration. *N Engl J Med*. 2006;355:1419–1431.
17. Miller RA, Oseroff AR, Stratte PT, Levy R. Monoclonal antibody therapeutic trials in seven patients with T-cell lymphoma. *Blood*. 1983;62:988–995.
18. Schroff RW, Foon KA, Beatty SM, Oldham RK, Morgan AC, Jr. Human anti-murine immunoglobulin responses in patients receiving monoclonal antibody therapy. *Cancer Res*. 1985;45:879–885.
19. Presta LG, Chen H, O'Connor SJ, et al. Humanization of an anti-vascular endothelial growth factor monoclonal antibody for the therapy of solid tumors and other disorders. *Cancer Res*. 1997;57:4593–4599.
20. Patil NS, Mihalache A, Dhoot AS, Popovic MM, Muni RH, Kertes PJ. Association between visual acuity and residual retinal fluid following intravitreal anti-vascular endothelial growth factor treatment for neovascular age-related macular degeneration: a systematic review and meta-analysis. *JAMA Ophthalmol*. 2022;140:611–622.
21. Spini A, Giometto S, Donnini S, et al. Risk of intraocular pressure increase with intravitreal injections of vascular endothelial growth factor inhibitors: a cohort study. *Am J Ophthalmol*. 2022;248:45–50.
22. Stewart MW. Individualized treatment of neovascular age-related macular degeneration: what are patients gaining? Or losing? *J Clin Med*. 2015;4:1079–1101.
23. Zehden JA, Mortensen XM, Reddy A, Zhang AY. Systemic and ocular adverse events with intravitreal anti-VEGF therapy used in the treatment of diabetic retinopathy: a review. *Curr Diab Rep*. 2022;22:525–536.
24. Bakri SJ, Snyder MR, Reid JM, Pulido JS, Singh RJ. Pharmacokinetics of intravitreal bevacizumab (Avastin). *Ophthalmology*. 2007;114:855–859.
25. Pearce I, Banerjee S, Burton BJ, et al. Ranibizumab 0.5 mg for diabetic macular edema with bimonthly monitoring after a phase of initial treatment: 18-month, multicenter, phase IIIB RELIGHT study. *Ophthalmology*. 2015;122:1811–1819.
26. Pearce W, Hsu J, Yeh S. Advances in drug delivery to the posterior segment. *Curr Opin Ophthalmol*. 2015;26:233–239.
27. Peyman GA, Lad EM, Moshfeghi DM. Intravitreal injection of therapeutic agents. *Retina*. 2009;29:875–912.
28. Thulliez M, Angoulvant D, Pisella PJ, Bejan-Angoulvant T. Overview of systematic reviews and meta-analyses on systemic adverse events associated with intravitreal anti-vascular endothelial growth factor medication use. *JAMA Ophthalmol*. 2018;136:557–566.
29. Fugara NA, Shawareb ZA, Rakkad NK, et al. The risk of non-arteritic ischemic optic neuropathy post-intravitreal bevacizumab injection. *Cureus*. 2022;14:e30185.
30. Iyer PG, Albini TA. Drug-related adverse effects of antivascular endothelial growth factor agents. *Curr Opin Ophthalmol*. 2021;32:191–197.
31. Maloney MH, Payne SR, Herrin J, Sangaralingham LR, Shah ND, Barkmeier AJ. Risk of systemic adverse events after intravitreal bevacizumab, ranibizumab, and aflibercept in routine clinical practice. *Ophthalmology*. 2021;128:417–424.
32. Agarwal A, Rhoades WR, Hanout M, et al. Management of neovascular age-related macular degeneration: current state-of-the-art care for optimizing visual outcomes and therapies in development. *Clin Ophthalmol*. 2015;9:1001–1015.
33. Chin-Yee D, Eck T, Fowler S, Hardi A, Apte RS. A systematic review of as needed versus treat and extend ranibizumab or bevacizumab treatment regimens for neovascular age-related macular degeneration. *Br J Ophthalmol*. 2016;100:914–917.
34. ElSheikh RH, Chauhan MZ, Sallam AB. Current and novel therapeutic approaches for treatment of neovascular age-related macular degeneration. *Biomolecules*. 2022;12:1629.
35. Garcia-Layana A, Figueroa MS, Arias L, et al. Individualized therapy with ranibizumab in wet age-related macular degeneration. *J Ophthalmol*. 2015;2015:412903.
36. Di Pierdomenico J, Garcia-Ayuso D, Jimenez-Lopez M, Agudo-Barriuso M, Vidal-Sanz M, Villegas-Perez MP. Different ipsi- and contralateral glial responses to anti-VEGF and triamcinolone intravitreal injections in rats. *Invest Ophthalmol Vis Sci*. 2016;57:3533–3544.
37. Filek R, Hooper P, Sheidow TG, Liu H, Chakrabarti S, Hutnik CM. Safety of anti-VEGF treatments in a diabetic rat model and retinal cell culture. *Clin Ophthalmol*. 2019;13:1097–1114.
38. Bhisitkul RB, Mendes TS, Rofagha S, et al. Macular atrophy progression and 7-year vision outcomes in subjects from the ANCHOR, MARINA, and HORIZON studies: the SEVEN-UP study. *Am J Ophthalmol*. 2015;159:915–924.e912.
39. SooHoo JR, Seibold LK, Kahook MY. Recent advances in the management of neovascular glaucoma. *Semin Ophthalmol*. 2013;28:165–172.
40. Uludag G, Hassan M, Matsumiya W, et al. Efficacy and safety of intravitreal anti-VEGF therapy in diabetic retinopathy: what we have learned and what should we learn further? *Expert Opin Biol Ther*. 2022;22:1275–1291.
41. Caceres-Del-Carpio J, Moustafa MT, Toledo-Corral J, et al. In vitro response and gene expression of human retinal Muller cells treated with different anti-VEGF drugs. *Exp Eye Res*. 2020;191:107903.
42. Matsuda M, Krempel PG, Marquezini MV, et al. Cellular stress response in human Muller cells (MIO-M1) after bevacizumab treatment. *Exp Eye Res*. 2017;160:1–10.
43. Ramon D, Shahar J, Massarweh A, Man I, Perlman I, Loewenstein A. Retinal toxicity of intravitreal injection of Ziv-aflibercept in albino rabbits. *Transl Vis Sci Technol*. 2018;7:23.
44. Gaddini L, Varano M, Matteucci A, et al. Muller glia activation by VEGF-antagonizing drugs: an in vitro study on rat primary retinal cultures. *Exp Eye Res*. 2016;145:158–163.

Investigative Ophthalmology & Visual Science

45. da Silva RA, Ferreira LPS, Roda VMP, Soares Junior JM, Simoes MJ, Regatieri CVS. Do anti-VEGFs used in the ophthalmic clinic cause Muller glial cell stress? *Clinics (Sao Paulo)*. 2023;78:100161.
46. Cheng CK, Peng PH, Tien LT, Cai YJ, Chen CF, Lee YJ. Bevacizumab is not toxic to retinal ganglion cells after repeated intravitreal injection. *Retina*. 2009;29:306–312.
47. Iriyama A, Chen YN, Tamaki Y, Yanagi Y. Effect of anti-VEGF antibody on retinal ganglion cells in rats. *Br J Ophthalmol*. 2007;91:1230–1233.
48. Seitz R, Tamm ER. Muller cells and microglia of the mouse eye react throughout the entire retina in response to the procedure of an intravitreal injection. *Adv Exp Med Biol*. 2014;801:347–353.
49. Thaler S, Fiedorowicz M, Choragiewicz TJ, et al. Toxicity testing of the VEGF inhibitors bevacizumab, ranibizumab and pegaptanib in rats both with and without prior retinal ganglion cell damage. *Acta Ophthalmol*. 2010;88:e170–176.
50. Di Pierdomenico J, Gallego-Ortega A, Martinez-Vacas A, et al. Intravitreal and subretinal syngeneic bone marrow mononuclear stem cell transplantation improves photoreceptor survival but does not ameliorate retinal function in two rat models of retinal degeneration. *Acta Ophthalmol*. 2022;100:e1313–e1331.
51. Di Pierdomenico J, Garcia-Ayuso D, Rodriguez Gonzalez-Herrero ME, et al. Bone marrow-derived mononuclear cell transplants decrease retinal gliosis in two animal models of inherited photoreceptor degeneration. *Int J Mol Sci*. 2020;21:7252.
52. Di Pierdomenico J, Scholz R, Valiente-Soriano FJ, et al. Neuroprotective effects of FGF2 and minocycline in two animal models of inherited retinal degeneration. *Invest Ophthalmol Vis Sci*. 2018;59:4392–4403.
53. Sebag J, Balazs EA. Morphology and ultrastructure of human vitreous fibers. *Invest Ophthalmol Vis Sci*. 1989;30:1867–1871.
54. Dureau P, Bonnel S, Menasche M, Dufier JL, Abitbol M. Quantitative analysis of intravitreal injections in the rat. *Curr Eye Res*. 2001;22:74–77.
55. Vezina M, Bussieres M, Glazier G, Gagnon M-P, Martel D. Determination of injectable intravitreous volumes in rats. *Invest Ophthalmol Vis Sci*. 2011;52:3219.
56. Di Pierdomenico J, Martinez-Vacas A, Hernandez-Munoz D, et al. Coordinated intervention of microglial and muller cells in light-induced retinal degeneration. *Invest Ophthalmol Vis Sci*. 2020;61:47.
57. Garcia-Ayuso D, Di Pierdomenico J, Hadj-Said W, et al. Taurine depletion causes ipRGC loss and increases light-induced photoreceptor degeneration. *Invest Ophthalmol Vis Sci*. 2018;59:1396–1409.
58. Garcia-Ayuso D, Di Pierdomenico J, Valiente-Soriano FJ, et al. beta-alanine supplementation induces taurine depletion and causes alterations of the retinal nerve fiber layer and axonal transport by retinal ganglion cells. *Exp Eye Res*. 2019;188:107781.
59. Garcia-Ayuso D, Di Pierdomenico J, Esquiva G, et al. Inherited photoreceptor degeneration causes the death of melanopsin-positive retinal ganglion cells and increases their coexpression of Brn3a. *Invest Ophthalmol Vis Sci*. 2015;56:4592–4604.
60. Garcia-Ayuso D, Salinas-Navarro M, Agudo M, et al. Retinal ganglion cell numbers and delayed retinal ganglion cell death in the P23H rat retina. *Exp Eye Res*. 2010;91:800–810.
61. Nadal-Nicolas FM, Jimenez-Lopez M, Sobrado-Calvo P, et al. Brn3a as a marker of retinal ganglion cells: qualitative and quantitative time course studies in naive and optic nerve-injured retinas. *Invest Ophthalmol Vis Sci*. 2009;50:3860–3868.
62. Di Pierdomenico J, Garcia-Ayuso D, Pinilla I, et al. Early events in retinal degeneration caused by rhodopsin mutation or pigment epithelium malfunction: differences and similarities. *Front Neuroanat*. 2017;11:14.
63. Martinez-Vacas A, Di Pierdomenico J, Valiente-Soriano FJ, et al. Glial cell activation and oxidative stress in retinal degeneration induced by beta-alanine caused taurine depletion and light exposure. *Int J Mol Sci*. 2021;23:346.
64. Valiente-Soriano FJ, Di Pierdomenico J, Garcia-Ayuso D, et al. Pigment epithelium-derived factor (PEDF) fragments prevent mouse cone photoreceptor cell loss induced by focal phototoxicity in vivo. *Int J Mol Sci*. 2020;21:7242.
65. Garcia-Ayuso D, Galindo-Romero C, Di Pierdomenico J, Vidal-Sanz M, Agudo-Barriuso M, Villegas Perez MP. Light-induced retinal degeneration causes a transient down-regulation of melanopsin in the rat retina. *Exp Eye Res*. 2017;161:10–16.
66. Garcia-Ayuso D, Salinas-Navarro M, Nadal-Nicolas FM, et al. Sectorial loss of retinal ganglion cells in inherited photoreceptor degeneration is due to RGC death. *Br J Ophthalmol*. 2014;98:396–401.
67. Galindo-Romero C, Jimenez-Lopez M, Garcia-Ayuso D, et al. Number and spatial distribution of intrinsically photosensitive retinal ganglion cells in the adult albino rat. *Exp Eye Res*. 2013;108:84–93.
68. Salinas-Navarro M, Mayor-Torroglosa S, Jimenez-Lopez M, et al. A computerized analysis of the entire retinal ganglion cell population and its spatial distribution in adult rats. *Vision Res*. 2009;49:115–126.
69. Kohen MC, Tatlipinar S, Cumbul A, Uslu U. The effects of bevacizumab treatment in a rat model of retinal ischemia and perfusion injury. *Mol Vis*. 2018;24:239–250.
70. Xiao A, Zhou Q, Shao Y, Zhong HF. Effect of intravitreal injection of ranibizumab on retinal ganglion cells and microvessels in the early stage of diabetic retinopathy in rats with streptozotocin-induced diabetes. *Exp Ther Med*. 2017;13:3360–3368.
71. Joachim SC, Renner M, Reinhard J, et al. Protective effects on the retina after ranibizumab treatment in an ischemia model. *PLoS One*. 2017;12:e0182407.
72. Guo L, Choi S, Bikkannavar P, Cordeiro MF. Microglia: key players in retinal ageing and neurodegeneration. *Front Cell Neurosci*. 2022;16:804782.
73. Martinez-Vacas A, Di Pierdomenico J, Gallego-Ortega A, et al. Systemic taurine treatment affords functional and morphological neuroprotection of photoreceptors and restores retinal pigment epithelium function in RCS rats. *Redox Biol*. 2022;57:102506.
74. Di Pierdomenico J, Garcia-Ayuso D, Agudo-Barriuso M, Vidal-Sanz M, Villegas-Perez MP. Role of microglial cells in photoreceptor degeneration. *Neural Regen Res*. 2019;14:1186–1190.
75. Pinilla I, Maneu V, Campello L, et al. Inherited Retinal Dystrophies: Role of Oxidative Stress and Inflammation in Their Physiopathology and Therapeutic Implications. *Antioxidants (Basel)*. 2022;11:1086.
76. Trouillet A, Dubus E, Degardin J, et al. Cone degeneration is triggered by the absence of USH1 proteins but prevented by antioxidant treatments. *Sci Rep*. 2018;8:1968.
77. Park SC, Su D, Tello C. Anti-VEGF therapy for the treatment of glaucoma: a focus on ranibizumab and bevacizumab. *Expert Opin Biol Ther*. 2012;12:1641–1647.
78. Couturier A, Bousquet E, Zhao M, et al. Anti-vascular endothelial growth factor acts on retinal microglia/macrophage activation in a rat model of ocular inflammation. *Mol Vis*. 2014;20:908–920.

Investigative Ophthalmology & Visual Science

79. Chang ML, Wu CH, Chien HF, Jiang-Shieh YF, Shieh JY, Wen CY. Microglia/macrophages responses to kainate-induced injury in the rat retina. *Neurosci Res*. 2006;54:202–212.
80. Palmhof M, Lohmann S, Schulte D, et al. Fewer functional deficits and reduced cell death after ranibizumab treatment in a retinal ischemia model. *Int J Mol Sci*. 2018;19:1636.
81. Lim SW, Bandala-Sanchez E, Kolic M, et al. The influence of intravitreal ranibizumab on inflammation-associated cytokine concentrations in eyes with diabetic macular edema. *Invest Ophthalmol Vis Sci*. 2018;59:5382–5390.
82. Mastropasqua R, D'Aloisio R, Di Nicola M, et al. Relationship between aqueous humor cytokine level changes and retinal vascular changes after intravitreal aflibercept for diabetic macular edema. *Sci Rep*. 2018;8:16548.
83. Motohashi R, Noma H, Yasuda K, Kotake O, Goto H, Shimura M. Dynamics of inflammatory factors in aqueous humor during ranibizumab or aflibercept treatment for age-related macular degeneration. *Ophthalmic Res*. 2017;58:209–216.
84. Noma H, Mimura T, Yasuda K, Motohashi R, Kotake O, Shimura M. Aqueous humor levels of soluble vascular endothelial growth factor receptor and inflammatory factors in diabetic macular edema. *Ophthalmologica*. 2017;238:81–88.
85. Raczynska D, Lisowska KA, Pietruczuk K, et al. The level of cytokines in the vitreous body of severe proliferative diabetic retinopathy patients undergoing posterior vitrectomy. *Curr Pharm Des*. 2018;24:3276–3281.
86. Pongsachareonnont P, Mak MYK, Hurst CP, Lam WC. Neovascular age-related macular degeneration: intraocular inflammatory cytokines in the poor responder to ranibizumab treatment. *Clin Ophthalmol*. 2018;12:1877–1885.
87. Tschulakow A, Christner S, Julien S, Ludinsky M, van der Giet M, Schraermeyer U. Effects of a single intravitreal injection of aflibercept and ranibizumab on glomeruli of monkeys. *PLoS One*. 2014;9:e113701.
88. Schnichels S, Hagemann U, Januschowski K, et al. Comparative toxicity and proliferation testing of aflibercept, bevacizumab and ranibizumab on different ocular cells. *Br J Ophthalmol*. 2013;97:917–923.
89. Cuenca N, Fernandez-Sanchez L, Campello L, et al. Cellular responses following retinal injuries and therapeutic approaches for neurodegenerative diseases. *Prog Retin Eye Res*. 2014;43:17–75.
90. Ellis-Behnke RG, Jonas RA, Jonas JB. The microglial system in the eye and brain in response to stimuli in vivo. *J Glaucoma*. 2013;22(Suppl 5):S32–S35.
91. Park HY, Kim JH, Park CK. Neuronal cell death in the inner retina and the influence of vascular endothelial growth factor inhibition in a diabetic rat model. *Am J Pathol*. 2014;184:1752–1762.
92. Cam D, Berk AT, Micili SC, Kume T, Ergur BU, Yilmaz O. Histological and immunohistochemical retinal changes following the intravitreal injection of aflibercept, bevacizumab and ranibizumab in newborn rabbits. *Curr Eye Res*. 2017;42:315–322.
93. Cui Q, Ren C, Sollars PJ, Pickard GE, So KF. The injury resistant ability of melanopsin-expressing intrinsically photosensitive retinal ganglion cells. *Neuroscience*. 2015;284:845–853.
94. Valiente-Soriano FJ, Salinas-Navarro M, Jimenez-Lopez M, et al. Effects of ocular hypertension in the visual system of pigmented mice. *PLoS One*. 2015;10:e0121134.
95. Vugler A, Semo M, Ortin-Martinez A, et al. A role for the outer retina in development of the intrinsic pupillary light reflex in mice. *Neuroscience*. 2015;286:60–78.
96. Valiente-Soriano FJ, Nadal-Nicolas FM, Salinas-Navarro M, et al. BDNF rescues RGCs but not intrinsically photosensitive RGCs in ocular hypertensive albino rat retinas. *Invest Ophthalmol Vis Sci*. 2015;56:1924–1936.
97. Di Pierdomenico J, Henderson DCM, Giammaria S, et al. Age and intraocular pressure in murine experimental glaucoma. *Prog Retin Eye Res*. 2022;88:101021.
98. Fleckenstein M, Schmitz-Valckenberg S, Chakravarthy U. Age-related macular degeneration: a review. *JAMA*. 2024;331:147–157.
99. Pham B, Thomas SM, Lillie E, et al. Anti-vascular endothelial growth factor treatment for retinal conditions: a systematic review and meta-analysis. *BMJ Open*. 2019;9:e022031.

Investigative Ophthalmology & Visual Science